Emission-Depth-Selective Auger Photoelectron Coincidence Spectroscopy

Wolfgang S. M. Werner, Werner Smekal, Herbert Störi, and Hannspeter Winter
Institut für Allgemeine Physik, Vienna University of Technology, Wiedner Hauptstraße 8-10, A-1040 Vienna, Austria

Giovanni Stefani, Alessandro Ruocco, and Francesco Offi
Dipartimento di Fisica and Unità INFM, Università di Roma Tre, via della Vasca Navale 84, I-00146 Rome, Italy

Roberto Gotter,[1] Alberto Morgante,[1,2] and Fernando Tommasini[1,2]
[1]*Laboratorio Nazionale TASC-INFM, Area Science Park, SS14 km 163.5, I-34012 Trieste, Italy*
[2]*Dipartimento di Fisica, Università di Trieste, via Valerio 2, I-34127 Trieste, Italy*
(Received 26 July 2004; published 27 January 2005)

The collision statistics of the energy dissipation of Auger and photoelectrons emitted from an amorphized Si(100) surface is studied by measuring the Si $2p$ photoelectron line as well as the first plasmon loss peak in coincidence with the Si-LVV Auger transition and the associated first plasmon loss. The Si $2p$ plasmon intensity decreases when measured in coincidence with the Si-LVV peak. If measured in coincidence with the Si-LVV plasmon the decrease is significantly smaller. The results agree quantitatively with calculations accounting for surface, volume, and intrinsic losses as well as elastic scattering in a random medium. In this way one can determine the average emission depth of *individual* electrons by means of Auger photoelectron coincidence spectroscopy, which therefore constitutes a unique tool to investigate interfaces at the nanoscale level.

DOI: 10.1103/PhysRevLett.94.038302 PACS numbers: 82.80.Pv, 68.49.Jk, 79.60.–i

In the past decades electron spectroscopy has found widespread application for investigating the electronic, structural and magnetic properties of materials in various aggregation states. In condensed matter, the strong electron-solid interaction gives rise to a small electron inelastic mean free path (up to several tens of an Å), resulting in the high surface sensitivity of the technique [1]. By changing the photoelectron kinetic energy and take-off angle, the average probing depth can be varied. However, it is not possible in this way to directly determine the photoelectron escape depth with a resolution better than the mean free path. This poses severe restrictions for calibrating the depth scale of nanosystems where a depth resolution significantly smaller than the electron mean free path is of great interest [2,3].

In Auger photoelectron coincidence spectroscopy (APECS), photoelectrons are measured in coincidence with Auger electrons emitted from the same ionization event. This allows one to study the emission process in greater detail, permitting the identification of initial and final state effects, satellite structures, shake processes, etc. [4–10]. In early work in this field [4], it was already pointed out that the surface sensitivity of the technique is enhanced as compared to ordinary electron spectroscopy, manifest in a decreased inelastic background in the experimental spectra [5,6].

A quantitative model for the surface sensitivity of APECS has been put forward [11], in which it was shown that the surface sensitivity of the technique can be varied by measuring the photoelectron peak in coincidence with the loss features accompanying the main Auger line, and vice versa. A first successful test of this model for the coincident (peak-peak) angular distribution was carried out recently [12]. In the present Letter, peak-peak and peak-plasmon coincidences of the Si $2p$ core-hole spectra emitted from an Si(100) surface (amorphized by ion bombardment) are reported. The theory for the surface sensitivity [11] is quantitatively verified and the ability of APECS to determine the average emission depth of *individual* Auger and photoelectrons is demonstrated. This makes the technique a unique tool to investigate interfaces at the nanoscale level.

Within the framework of a linearized Boltzmann-type kinetic equation [1,13,14], the emerging spectrum may be assumed to consist of groups of electrons that have experienced a certain number of inelastic collisions of different kinds (bulk, surface, or intrinsic excitations). The energy fluctuations within each group are given by multiple convolutions of the energy loss distribution in an individual excitation. The collision statistics are described by the so-called partial intensities, i.e., the number of electrons within a given group of n-fold inelastically scattered electrons. For surface and intrinsic excitations these quantities are commonly assumed to follow Poisson statistics. The extrinsic partial intensities for bulk scattering, C_{n_b}, depend on the elastic as well as the inelastic interaction and can be established by numerical calculations [15]. An example is shown in Figs. 1(a) and 1(b)that display the escape probability of the Si $2p$ [$\phi_{n_X}(z)$] and Si-LVV [$\phi_{n_A}(z)$] electrons which have experienced a certain number of volume excitations.

The corresponding total number of escaping electrons is derived from the area under these curves. In the case of APECS, one is only interested in electrons created at the

 © 2005 The American Physical Society

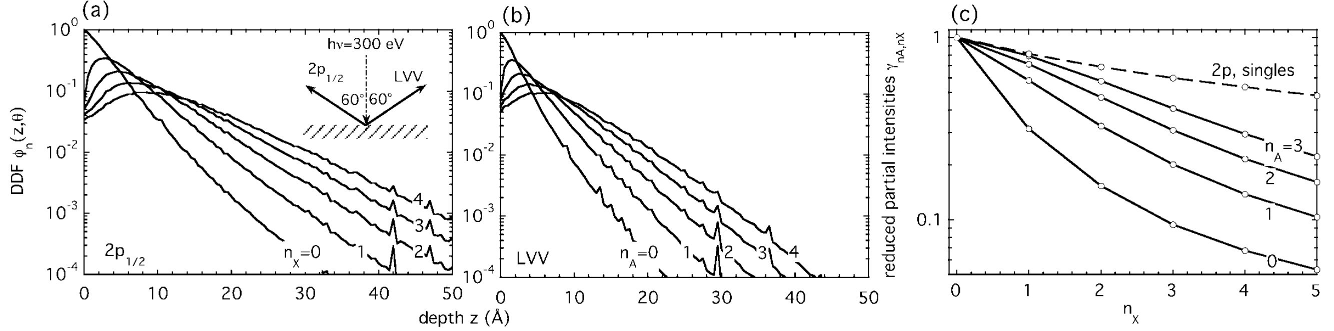

FIG. 1. (a) Partial escape distribution, or depth distribution function (DDF), $\phi_{n_X}(z, \theta_o)$ for the Si $2p_{1/2}$ transition. These data were simulated by means of a Monte Carlo model [15] for normal x-ray incidence, and with the Auger and photoelectron detected at an off-normal emission angle of 60°, as indicated in the inset. (b) Same as (a), for Si-*LVV* Auger electrons. (c) Reduced double differential partial intensities for bulk inelastic scattering $\gamma_{n_X,n_A} = C_{n_X,n_A}/C_{n_X=0,n_A=0}$ calculated from the curves in (a) and (b) using Eq. (1). The dashed curve represents the Si $2p$ singles partial intensities for bulk scattering.

same location, and the partial intensities for APECS for an ideally flat homogeneous surface can be written as

$$C_{n_A,n_X} = \int_0^\infty \phi_{n_X}(z)\phi_{n_A}(z)dz, \qquad (1)$$

where n_X and n_A denote the collision number of the photoelectron and Auger electron, respectively. A survey of the collision statistics for the Si $2p$ APECS core-hole spectrum is presented in Fig. 1(c), which displays the partial intensities normalized by the elastic peak area. If the Si $2p$ peak is measured in coincidence with the *LVV* no-loss peak (curve labeled $n_A = 0$), the first and higher order plasmons ($n_X \geq 1$) are strongly reduced with respect to the singles spectrum (dashed line). If the same spectrum is measured in coincidence with the first plasmon in the Auger line ($n_A = 1$), the intensity of the inelastic background increases again. Since the probability for inelastic scattering increases monotonically with the respective path length, those Auger electrons that end up in the first plasmon peak originate from larger depths. Then the $2p$ electrons measured in coincidence with them will also travel a longer path length in the solid and the probability for experiencing an inelastic collision increases. An estimate for the average emission depth in the rectilinear motion model ignoring surface and intrinsic excitations yields

$$\langle z \rangle_{n_X,n_A} = (n_A + n_X + 1)\frac{\mu_A \mu_X}{\mu_A + \mu_X}, \qquad (2)$$

where $\mu_{A,X} = \lambda_{A,X}\cos\theta_{A,X}$, λ denotes the inelastic mean free path, and θ represents the emission angle. Thus the emission depth of the elastic peak in the photoelectron spectrum ($n_X = 0$) can be selected by measuring the spectrum in coincidence with energies corresponding to a particular number of plasmon losses in the Auger line. For common electron spectroscopy, the photoelectrons in the elastic peak always originate from the same average depth $\langle z \rangle = \mu_X$. This illustrates the ability of APECS to select the average electron emission depth. In the present Letter, the collision statistics have been investigated for $n_A = 0, 1$ and $n_X = 0, 1$ by measuring the related peak-peak, peak-plasmon, and plasmon-plasmon coincidences.

A Si(100) sample was cut from a wafer of lightly doped Si ($10^{15} P$ atoms cm^{-3}), mounted in the chamber of the ALOISA beam line at ELETTRA (base pressure 3×10^{-10} mbar) [16], and subjected to repeated cycles of annealing at 1100 °C and 3 keV Ar^+ sputtering. After this treatment the C and O contamination levels were below 10% of a monolayer and the resulting surface was completely amorphized to sufficiently large depths, as verified by x-ray photoemission spectroscopy (XPS) angle scans that exhibited no diffraction effects. During the coincidence measurements the cleaning procedure was repeated at every injection of electrons in the ring, which took place every ~24 h. Singles spectra measured as a reference at $h\nu = 300$ eV were subjected to a partial intensity analysis [1,13,17]. This was done to eliminate multiple scattered electrons and to determine the peak parameters and gain information on the intrinsic and surface excitation probabilities needed in the simulation of the APECS spectra.

As an example, Fig. 2 shows the Si-*LVV* peak as measured (dash-dotted line) and after line shape analysis (data points). The background subtracted spectrum was fitted by three Gaussians. These three components compare well with the assignment of Pernaselci and Cini [18] who calculated the Si-*LVV* and Si-*KVV* line shapes by means of an extended Cini-Sawatzky theory. Thus the dashed curves are identified as the self-convolution of the p-state electronic density of states (p-DOS), while the dotted curve corresponds to the convolution of the s- and p-DOS. The intensity ratio of the sp- and pp-contributions of our results is 0.30 ± 0.05, close to the value of 0.38 ± 0.02, as quoted in Ref. [19]. The background subtracted Si $2p$ spectrum was fitted to a linear combination of two Doniach-Sunjic line shapes with a fixed doublet ratio of $I_{2p_{3/2}}/I_{2p_{1/2}} = 2$. The separation between the $2p_{1/2}$ and $2p_{3/2}$ component was 0.6 eV, in good agreement with earlier assessments [20].

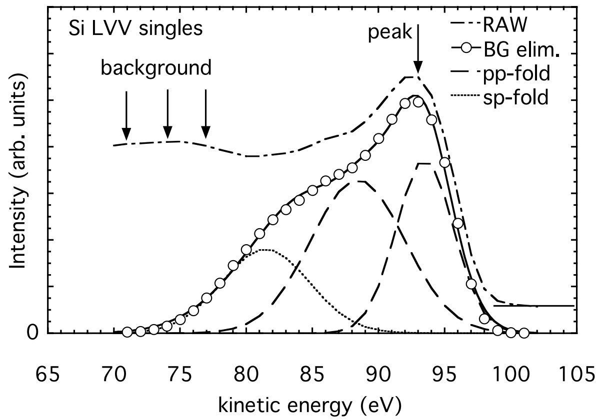

FIG. 2. Experimental Si-LVV singles spectrum [15] (dash-dotted line). The same spectrum subjected to a Partial Intensity Analysis [1,13,17] is represented by open circles.

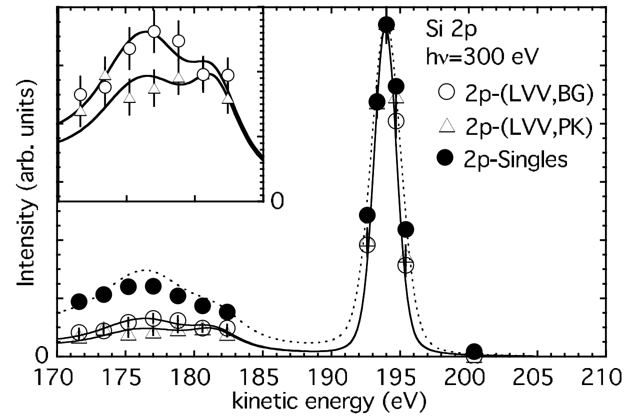

FIG. 3. Si $2p$ spectrum measured in coincidence with the background in the Si-LVV spectrum (open circles, see arrows marked "background" in Fig. 2), as well as with the peak of the Si-LVV Auger line (open triangles, arrow marked "peak" in Fig. 2). The filled circles are the corresponding singles intensities. The solid and dotted lines represent results of model calculations with the SESSA software (Simulation of Electron Spectra for Surface Analysis) [15] (see text). The data were normalized at the peak maximum. The inset shows an expanded view of the BG and PK spectra.

Subsequently, Si $2p$ electrons detected in the two bimodal analyzers (energy resolution $\Delta E = 2.2$ eV) of the ALOISA apparatus were measured in coincidence with Auger electrons arriving in the five axial analyzers ($\Delta E = 3$ eV) [16]. The photon beam intensity was decreased by reducing the monochromator slit width to give a true to random coincidence ratio of approximately one in the peak-peak coincidences. For the coincidence measurements the sample surface normal was in the plane of incidence of the incoming (linearly polarized) light and the polarization vector. The angle between the sample surface normal and the incidence direction of the light was chosen to be 72°, well below the critical angle for total reflection of ~84° at $h\nu = 300$ eV. The bimodal analyzers that were also in the plane of incidence were oriented at emission angles of 2° and 20° relative to the surface normal. The plane of the axial analyzers was tilted 35° with respect to the plane of incidence.

Two of the axial analyzers were tuned to the no-loss Auger peak, while the other three measured the intensity at the first plasmon loss, as indicated by the arrows in Fig. 2. After data acquisition, the spectra recorded in coincidence with the LVV peak and plasmon loss were combined to yield the $2p$ spectra shown in Fig. 3 with the required statistics in the plasmon region. The energy range chosen for the $2p$ spectrum is shown in Fig. 3 and covers the no-loss peak and the first volume plasmon as well as a single point well above the peak, recorded as a reference. Data accumulation took place over a period of 6 d with an effective counting time of approximately 90 h.

The filled circles in Fig. 3 represent the singles spectra of the Si $2p$ region that are compared with the intensities measured in coincidence with the elastic peak (open triangles, referred to as "PK" hereafter) and the inelastic background (open circles, "BG") in the Si-LVV Auger electron line. All data shown in this figure are normalized to the same height in the peak maximum. The intensity of the plasmon in the PK spectrum is significantly reduced as compared to the singles spectrum, by about a factor of 2.5. This is a consequence of the well-known enhancement of the surface sensitivity of APECS as compared to ordinary XPS [4]. In the BG spectrum, the first plasmon intensity is higher, indicating that the path length the electrons travel inside the solid is longer, or in other words, that they originate from greater depths. These observations are qualitatively consistent with the theoretical considerations for the surface sensitivity discussed above. This can be seen in Fig. 1(c) where the corresponding partial intensities for the first volume plasmon in the singles spectrum (the point $n_X = 1$ in the curve labeled "$2p$, singles") is larger than for the BG spectrum ($\gamma_{n_X=1,n_A=1}$) while the latter is in turn larger than for the PK spectrum ($\gamma_{n_X=1,n_A=0}$). The experimental results therefore also provide direct proof for the existence of extrinsic plasmons that are independent from the atomic decay and (many-electron) relaxation processes involved in the photoelectron emission at the source.

For a quantitative comparison one has to account for elastic as well as intrinsic and surface inelastic collisions. Resulting simulated spectra [15] are shown in Fig. 3 as solid and dotted lines which agree quantitatively with the experimental data. The main uncertainty in the theoretical spectra is the intensity of the surface plasmon peak and the contribution of intrinsic excitations. However, even when surface and intrinsic excitations are completely disregarded in the simulation, the ratio of intensities of the first plasmon peak of the simulated BG and PK spectrum changes only by up to 15% and agrees with the measurements within the experimental uncertainty. Therefore we

conclude that the change of the plasmon intensity is a signature of the different depths sampled in the PK and BG spectrum and, most importantly, that the intensity of the elastic peak of these spectra is due to electrons with a different average emission depth: while the electrons in the PK spectrum originate from an average depth of about 2.0 ± 2.1 Å, the average emission depth of the BG spectrum amounts to about 4.7 ± 4.9 Å. The singles spectrum, on the other hand, consists of electrons emitted from an average depth of 6.1 ± 6.5 Å.

The uncertainties quoted above for the emission depths represent the root-mean-square widths $\sigma_{\langle z\rangle}$ of the fluctuations in the emission depth. In the rectilinear motion model, $\sigma_{\langle z\rangle}$ is equal to the average emission-depth $\langle z\rangle_0$, described by Eq. (2) for APECS, and equal to μ_X for ordinary XPS. A realistic estimate of the emission depth cannot be derived from a simple analytic formula, since it should account for all different scattering processes and also depends on the *shape* of the Auger and photoelectron peak, the shape of the inelastic cross section, and the energy interval in which the Auger and photoelectrons are accepted [11]. Furthermore, this formula neglects that a part of the electrons in the BG spectrum are measured in coincidence with the *intrinsic* plasmon of the LVV Auger line, which leads to an additional broadening of the emission-depth fluctuations since intrinsic excitations can take place at any depth. These phenomena have been accounted for in the values for $\sigma_{\langle z\rangle}$ presented above. It can therefore be stated that the present results prove the ability of APECS to discriminate the average emission depth of individual electrons within the limits of the statistical fluctuations of the emission depth that are inherent to the stochastic process for multiple scattering.

Another interesting feature seen in Fig. 3 is the change in the linewidth of the coincidence spectra as compared to the singles spectrum. The simulated spectra match the experimental linewidth by allowing for a narrowing of the linewidth of the coincidence spectra by 0.8 eV, taking into account the experimental broadening of 1.1 eV. The fact that our measurement comprises the unresolved $2p_{1/2}$ and $2p_{3/2}$ components makes the interpretation of this observation difficult. However, it is noted that the line narrowing seems to be symmetric, indicating that both core-hole components are indeed present also in the coincidence spectra.

It was already anticipated [4] that APECS can be used to remove the core-hole lifetime broadening and modify other contributions to line broadening. Indeed, line narrowing in photoemission spectra by APECS has been observed by several groups [7,10] and is a clear indication for the one-step character of the Auger emission process [21]. The present observation adds to the body of evidence for this statement but on the basis of the experimental energy resolution and statistics it is difficult to decisively pinpoint the reason for this observation.

The authors are grateful to the ALOISA beam line staff for support during the experiments at ELETTRA. Partial support provided by the INFM project "Luce di Sincrotrone" is gratefully acknowledged. Two of the authors (W. S. M. W.) and (W. S.), gratefully acknowledge financial support of the present work by the Austrian Science Foundation FWF under Project No. P15938-N02 and the European Community-Research Infrastructure Action under the FP6 "Structuring the European Research Area" Programme (through the Integrated Infrastructure Initiative "Integrating Activity on Synchrotron and Free Electron Laser Science.

[1] W. S. M. Werner, in *Surface Analysis by Auger and X-Ray Photoelectron Spectroscopy*, edited by D. Briggs and J. Grant (IMPublications, Chichester, UK, 2003).
[2] I. Doron-Mor, A. Hatzor, A. Vaskevich, T. van der Boom-Moav, A. Shanzer, I. Rubinstein, and H. Cohen, Nature (London) **406**, 382 (2000).
[3] J. C. Lee, Appl. Phys. Lett. **84**, 3561 (2004).
[4] H. W. Haak, G. A. Sawatzky, and T. D. Thomas, Phys. Rev. Lett. **41**, 1825 (1978).
[5] E. Jensen, R. A. Bartynski, R. Garrett, S. L. Hulbert, E. D. Johnson, and C.-C. Kao, Phys. Rev. B **45**, 13 636 (1992).
[6] C. P. Lund and S. M. Thurgate, Phys. Rev. B **50**, 17 166 (1994).
[7] S. M. Thurgate and Z.-T. Jang, Surf. Sci. **466**, L807 (2000).
[8] S. M. Thurgate, Surf. Interface Anal. **20**, 627 (1993).
[9] E. Jensen, R. A. Bartynski, S. L. Hulbert, and E. D. Johnson, Rev. Sci. Instrum. **63**, 3013 (1992).
[10] E. Jensen, R. A. Bartynski, S. L. Hulbert, E. D. Johnson, and R. Garrett, Phys. Rev. Lett. **62**, 71 (1989).
[11] W. S. M. Werner, H. Störi, and HP. Winter, Surf. Sci. **518**, L569 (2002).
[12] A. Liscio, R. Gotter, A. Ruocco, S. Iacobucci, A. G. Danese, R. A. Bartynski, and G. Stefani, J. Electron Spectrosc. Relat. Phenom. **137**, 505 (2004).
[13] W. S. M. Werner and P. Schattschneider, J. Electron Spectrosc. Relat. Phenom. (to be published).
[14] W. S. M. Werner, Phys. Rev. B **55**, 14 925 (1997).
[15] W. S. M. Werner, W. Smekal, and C. J. Powell, *Simulation of Electron Spectra for Surface Analysis* (National Institute for Standards and Technology (NIST), Gaithersburg, Maryland, 2004).
[16] R. Gotter, A. Ruocco, A. Morgante, D. Cvetko, L. Floreano, F. Tommasini, and G. Stefani, Nucl. Instrum. Methods Phys. Res., Sect. A **467**, 1468 (2001).
[17] W. S. M. Werner, Surf. Interface Anal. **31**, 141 (2001).
[18] A. Pernaselci and M. Cini, J. Electron Spectrosc. Relat. Phenom. **82**, 79 (1996).
[19] D. E. Ramaker, F. L. Hutson, N. H. Turner, and W. N. Mei, Phys. Rev. B **33**, 2574 (1986).
[20] P. Unsworth, J. E. Evans, P. Weightman, A. Takahashi, J. A. D. Matthew, and Q. C. Herd, Phys. Rev. B **54**, 286 (1996).
[21] M. Ohno, J. Electron Spectrosc. Relat. Phenom. **124**, 53 (2002).